



Contents lists available at ScienceDirect

Bioorganic & Medicinal Chemistry Letters

journal homepage: www.elsevier.com/locate/bmcl

Discovery of spirocyclic secondary amine-derived tertiary ureas as highly potent, selective and bioavailable soluble epoxide hydrolase inhibitors

Hong C. Shen^{a,*}, Fa-Xiang Ding^a, Siyi Wang^a, Suoyu Xu^b, Hsuan-shen Chen^b, Xinchun Tong^b, Vincent Tong^b, Kaushik Mitra^b, Sanjeev Kumar^b, Xiaoping Zhang^c, Yuli Chen^c, Gaochao Zhou^c, Lee-Yuh Pai^d, Magdalena Alonso-Galicia^d, Xiaoli Chen^e, Bei Zhang^c, James R. Tata^a, Joel P. Berger^c, Steven L. Colletti^a

^a Department of Medicinal Chemistry, Merck Research Laboratories, PO Box 2000, Rahway, NJ 07065-0900, USA

^b Department of Drug metabolism, Merck Research Laboratories, PO Box 2000, Rahway, NJ 07065-0900, USA

^c Department of Metabolic Disorders, Merck Research Laboratories, PO Box 2000, Rahway, NJ 07065-0900, USA

^d Department of Cardiovascular Diseases, Merck Research Laboratories, PO Box 2000, Rahway, NJ 07065-0900, USA

^e Department of Pharmacology, Merck Research Laboratories, PO Box 2000, Rahway, NJ 07065-0900, USA

ARTICLE INFO

Article history:

Received 17 April 2009

Revised 7 May 2009

Accepted 11 May 2009

Available online 18 May 2009

Keywords:

Soluble epoxide hydrolase

sEH

Spirocyclic secondary amines

Spontaneously hypertensive rats

Tertiary ureas

ABSTRACT

Spirocyclic secondary amine-derived trisubstituted ureas were identified as highly potent, bioavailable and selective soluble epoxide hydrolase (sEH) inhibitors. Despite good oral exposure and excellent ex vivo target engagement in blood, one such compound, *rac*-**1a**, failed to lower blood pressure acutely in spontaneously hypertensive rats (SHRs). This study posed the question as to whether sEH inhibition provides a robust mechanism leading to a significant antihypertensive effect.

© 2009 Elsevier Ltd. All rights reserved.

Human soluble epoxide hydrolase (sEH, *EPHX2*) is a bifunctional and homodimer enzyme located in the cytosol and peroxisomes.¹ The highest specific activity of sEH is observed in liver, followed by kidney.² sEH mediates the metabolism of arachidonic acid and linoleic acid epoxides. Specifically, the C-terminus of sEH converts epoxyeicosatrienoic acids (EETs), which are derived from metabolism of arachidonic acid, to the corresponding dihydroxyeicosatrienoic acids (DHETs).³

EETs elicit a wide range of physiological effects.⁴ In particular, EETs display vasodilatory effects in conduit vessels, renal afferent arterioles, and coronary resistance vessels indicating a potential role of EETs in blood pressure regulation and myocardial perfusion.⁵ In rats, 14,15-EET transiently reduced arterial blood pressure.⁶ In addition to dilating coronary arteries and arterioles,⁷ EETs also modulate adhesion molecule expression, platelet aggregation, vascular smooth muscle migration, and thrombolytic properties thus representing a protective mechanism against

atherosclerosis.⁸ In ischemia-reperfusion injured rats, EETs have been shown to effectively reduce the myocardial infarct size.⁹

Therefore, the inhibition of sEH, as a strategy to elevate the levels of EETs, could have a significantly beneficial impact on diseases such as hypertension and atherosclerosis.¹ Recently, several sEH inhibitors have demonstrated a blood pressure lowering effect in an angiotensin II-induced hypertensive rat model.¹⁰ They also protected the rats' kidneys from hypertension-induced damage.¹¹ Arete has developed an sEH inhibitor for metabolic syndromes that will soon enter Phase II clinical trials.¹² These advancements prompted us to discover highly selective, orally bioavailable, and structurally novel sEH inhibitors for an antihypertensive indication.

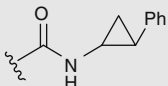
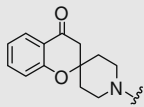
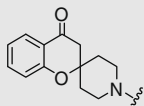
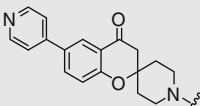
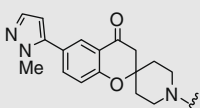
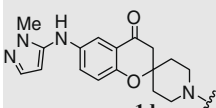
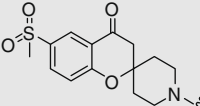
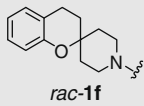
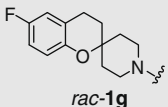
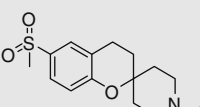
Our design of sEH inhibitors was informed by the X-ray crystal structure of sEH (1ZD3 (PDB code): human sEH 4-(3-cyclohexylureido)-butyric acid complex).¹³ It has been revealed that the hydrolytic catalytic site of sEH contains two tyrosine residues (Tyr381 and Tyr465) which act as hydrogen bond donors interacting with the epoxide oxygen of EETs, thereby facilitating the epoxide ring opening by Asp333. The resulting ester is then rapidly hydrolyzed into DHETs. Amides and ureas are excellent mimics of epoxides in that the amide or urea carbonyl oxygen acts as a hydrogen bond

* Corresponding author. Tel.: +1 732 594 1755; fax: +1 732 594 9473.

E-mail address: hong_shen@merck.com (H.C. Shen).

Table 1

In vitro SAR on sEH and mEH inhibition, DHET production, CYP and ion channel inhibitions

| Compds | sEH IC ₅₀ (h, r), nM ^a | DHET, IC ₅₀ , nM ^b | mEH, IC ₅₀ , μM ^c | CYP2C9, 2D6, 3A4 IC ₅₀ , μM | DLZ, IKr Na _v 1.5, IC ₅₀ , μM |
|--|--|--|---|--|---|
|  | | | | | |
|  entA-1a | 3, 9 | 3 | >100 | ~10, >10, >10 | >30, 14, >10 |
|  entB-1a | 11, 29 | 3 | >100 | >10, >10, >10 | >30, 17, >10 |
|  rac-1b | 1, 7 | — | >100 | <10, <10, <10 | 4, 0.2, >10 |
|  rac-1c | 4, 21 | <1 | 15 | >10, >10, >10 | 28, ^d 4, >10 |
|  rac-1d | 3, 13 | <1 | >100 | ~10, >10, >10 | 26, ^d 2, >10 |
|  rac-1e | 4, 12 | — | — | >10, >10, >10 | >26, 4, >10 |
|  rac-1f | 4, 11 | — | >100 | <10, >10, >10 | 6, 15, >10 |
|  rac-1g | 3, 18 | <1 | >100 | <10, >10, >10 | 2, 7, >10 |
|  ent-1h | 3, 23 | <1 | 24 | >10, >10, >10 | 28, 15, >10 |

(continued on next page)

Table 1 (continued)

| Compds | sEH IC ₅₀ (h, r), nM ^a | DHET, IC ₅₀ , nM ^b | mEH, IC ₅₀ , μM ^c | CYP2C9, 2D6, 3A4 IC ₅₀ , μM | DLZ, IKr Na _v 1.5, IC ₅₀ , μM |
|--------|--|--|---|--|---|
| | | | | | |
| | 11, 49 | 3 | 55 | >10, >10, >10 | >30, ^d 2, >10 |
| | 8, 20 | 4 | >100 | —, >10, >10 | >30, ^d >30, >10 |
| | 8, 31 | 8 | >100 | >10, >10, >10 | >30, >30, >10 |
| | 5, 21 | <1 | >100 | >10, >10, >10 | 20, ^d >30, >10 |

^a Values are based on one or two experiments, each in triplicate, and within 20% deviation upon repeat.

^b Studies were performed with HEK293 cells.

^c Human mEH was used.

^d Cav1.2 functional assay was performed.

acceptor for Tyr381 and Tyr465, whereas the hydrogen atom of amide or urea N–H group serves as a hydrogen bond donor to Asp333. Therefore, various ureas and amides have been developed as sEH inhibitors.¹⁴

We designed and prepared novel spirocyclic piperidine-based trisubstituted ureas as sEH inhibitors. Herein, we report the structure–activity relationship (SAR), off-target profiles, and target engagement of this class of compounds. Furthermore, we report data from a blood pressure study conducted in spontaneously hypertensive rats (SHRs), a common preclinical hypertension model that responds to various antihypertensive drugs.

To evaluate sEH inhibitors, human and rat sEH inhibition, and human whole cell DHET production were utilized to determine their intrinsic enzymatic and cellular activities. Counterscreening were routinely performed on microsomal epoxide hydrolase (mEH), several CYP enzymes and selected ion channels. Due to its important roles in xenobiotic detoxication and steroid metabolism, mEH inhibition was a key safety concern. Additionally, many ureas have been reported to inhibit this enzyme.¹⁵ Amongst the CYP2D6, 3A4, and 2C9 counterscreen targets, the latter is of particular importance due to its role in producing EETs via the monooxygenase-mediated epoxidation of arachidonic acid;³ CYP2C9 inhibition could result in a diminution in EET elevation. Lastly, effects of compounds on ion channels, including potassium (IKr), calcium (DLZ binding or Ca_v1.2 functional assays) and sodium (Na_v1.5) channels, were scrutinized due to their potential confounding cardiovascular effects.¹⁶ To the best of our knowledge, previous literature reports did not disclose their status of ion channel or CYP inhibitory effects. We strongly believe that a proper evaluation of the antihypertensive actions of sEH inhibitors should

be performed with compounds lacking any obvious off-target activity that could impact vascular tone.

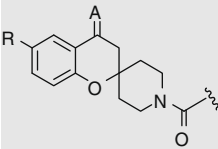
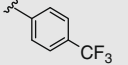
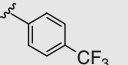
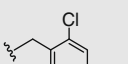
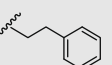
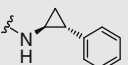
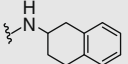
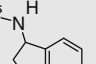
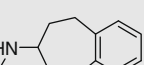
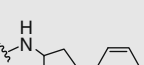
The SAR study was conducted in two directions including the left (Table 1) and right portion of the scaffold (Table 2) shown in brown and blue in Figure 1 respectively. Racemic compounds contain the prefix ‘rac’ while enantiomers are designated with ‘ent’.

In our first set of studies, the *trans*-2-phenyl-1-cyclopropylamino group was adopted as the common right-hand motif (Table 1). All compounds in Table 1 demonstrated excellent nanomolar IC₅₀s against the human sEH. In the rat sEH inhibition assay, compounds were typically 2–10-fold less active. The whole cell DHET assay results were in agreement with enzyme activity suggesting good cell permeability of compounds. A large window between sEH and mEH potency (>10,000-fold) was achieved for most analogs. In addition, ureas derived from one enantiomer of *trans*-2-phenyl-1-cyclopropylamine were consistently 3–8-fold more active than their enantiomeric counterparts, and both enantiomers gave very similar off-target profiles (data not shown).

The two enantiomers of **1a** were designated as *entA*-**1a** and *entB*-**1a**. Despite a threefold difference of the IC₅₀ in both human and rat sEH inhibition assays, they displayed similar off-target profiles and whole cell activity in DHET production inhibition. The chroman or chromanone moiety could be substituted with various groups ranging from heterocycles (**1b**, **1c**) and aminoheterocycles (**1d**) to halides (**1g**) and methylsulfone (**1e**) without compromising sEH potency. Unfortunately, these substitutions were found to introduce moderate potassium channel (IKr) activity. The replacement of chromanones with chromans did not significantly alter sEH IC₅₀s, but, in certain cases, ion channel activity was notably

Table 2

In vitro SAR on sEH and mEH inhibition, DHET production, CYP and ion channel inhibitions

| Compds | sEH IC ₅₀ (h, r), nM ^a | DHET, nM ^b | mEH, μM ^c | CYP2C9, 2D6, 3A4 IC ₅₀ , μM | DLZ, IKr Na _v 1.5, IC ₅₀ , μM |
|---|--|-----------------------|----------------------|--|---|
|  | | | | | |
|  2a R = H, A = H, H | 4, 10 | <1 | 22 | >10, >10, >10 | 2, 1, >10 |
|  2b R = SO ₂ Me, A = H, H | 2, 19 | <1 | >100 | 7.6, >10, >10 | >30, 25, >10 |
|  2c R = MeSO ₂ , A = H, H | 1, 4 | <1 | >100 | ~10, ~10, >10 | >30, 0.8, >10 |
|  2d R = F, A = H, H | 7, 10 | 3 | >100 | <10, <10, >10 | 3, 6, <10 |
|  <i>entA-1a</i> R = H, A = O | 3, 9 | 3 | >100 | ~10, >10, >10 | >30, 14, >10 |
|  <i>rac-2e</i> R = H, A = O | 5, 39 | — | 26 | >10, >10, >10 | 9, 12, ~1 |
|  <i>rac-2f</i> R = H, A = O | 20, 35 | 30 | 28 | <10, >10, >10 | 6, 6, <10 |
|  <i>rac-2g</i> R = H, A = O | 8, 28 | — | >100 | <10, >10, <10 | 5, 5, <10 |
|  <i>rac-1,3-trans-2h</i> R = SO ₂ Me, A = O | 7, 21 | — | 10 | <10, >10, >10 | 18, 3, >10 |

^a Values are based on one or two experiments, each in triplicate, and within 20% deviation upon repeat.^b Studies were performed with HEK293 cells.^c Human mEH was used.

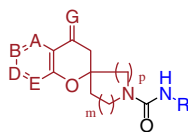


Figure 1. Pharmacophore of urea analogs.

changed. For example, the DLZ binding affinity of chroman **1f** was higher than either chromanone *entA-1a* or *entB-1a*. On the other hand, the IKr activity of chroman **1h** was less than that of chromanone **1e**. The piperidine moiety could be replaced by a homopiperidine group, accompanied by a significant increase of IKr activity (**1i**). Lastly, the replacement of chroman benzene moiety with pyridine, shown in analogs **1j–l**, provided excellent enzyme and whole cell sEH inhibition, yet devoid of significant off-target activity against CYPs and ion channels. The pyridine regioisomers shown in **1j–l** provided at least a threefold greater potency of sEH inhibition than the other three regioisomers (data not shown).

In subsequent studies, the right fragment (in blue) of the urea structure shown in Figure 1 was probed. After screening a variety of primary amines or anilines, it was found that phenyl cyclopropyl amine (*ent-1a*) gave the best overall profile, on the basis of sEH, CYP, DLZ and IKr activities.

To prioritize compounds for in vivo PD studies, an in vitro DHET production assay was conducted in which each of the compounds was incubated in rat blood for 1 h before the addition of substrate (14,15-EET) and the measurement of DHET production rate. Despite similar enzymatic and cellular activity, inhibitors were differentiated in this assay, presumably reflecting their differential affinity for blood proteins. Compounds *rac-1a*, *ent-1j*, *ent-1k* and *ent-1l* clearly exhibited more potent inhibition of DHET production than analogs *rac-1f*, *rac-1h*, **2a** and **2b** (Table 3).

The pharmacokinetic (PK) profiles of five analogs in rats are presented in Table 4. Excellent bioavailability, moderate to good half life, and good to excellent oral exposure were observed for all compounds. In addition, most compounds displayed low clearance except *rac-1a*. Despite the inferior PK of compound *rac-1a* reflected by its relatively lower oral exposure and higher clearance, the excellent whole blood activity of *rac-1a* seemed to indicate that this compound had a good free fraction in plasma. The high free fraction of *rac-1a* could account for its higher apparent clearance. Therefore, compound *rac-1a* was selected for an ex vivo target engagement evaluation. In this study, SHR_s were treated with

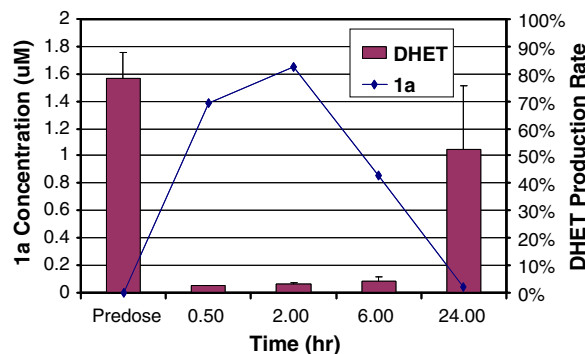


Figure 2. Ex vivo whole blood target engagement of *rac-1a* measured by 14,15-DHET production (50 mpk, po).

rac-1a at a 50 mpk dose (po). At 0 h, 0.5 h, 2 h, 6 h and 24 h, blood was drawn and combined with 14,15-EET; 14,15-DHET and the compound concentration was then assayed. An excellent inverse correlation was established between the plasma level of *rac-1a* and DHET production (Fig. 2). The drug level remained above 0.8 µM and DHET production was suppressed >95% from 0.5–6 h post dose.

At a 300 mpk oral dose, which should presumably provide even more substantial sEH engagement than demonstrated above at 50 mpk, *rac-1a* failed to induce statistically significant change of systolic or diastolic blood pressure in SHR_s (Fig. 3). A parallel one-day PK study at 300 mpk dose showed that the drug level of *rac-1a* remained above 1.7 µM during the period of 2–24 h post dosing (3.6 µM at 2 h, 2.7 µM at 5 h, and 1.7 µM at 24 h). Based on the whole blood target engagement results depicted in Figure 2, the DHET production in blood should be reduced more than 95% compared with the control group throughout the PD study timeframe.

Heart rate and pulse pressure differences between the treated and vehicle (labrasol) groups were also negligible (Fig. 3).

The representative synthesis of a spirocyclic secondary amine-derived urea is shown in Scheme 1.¹⁷ An efficient one-step conversion of carboxylic acid **3** into methyl ketone **4**, followed by a pyrrolidine-mediated spirocyclization afforded intermediate **6**. The ketone group in **6** was then reduced to CH₂ via a reduction, dehydration, and hydrogenation sequence. The resulting amine **9** reacted with the *p*-nitrophenyl carbamate generated in situ from the phenyl cyclopropyl amine enantiomer **10** (i.e., the enantiomer

Table 3
In vitro DHET production in whole rat blood^a

| Compd | <i>rac-1a</i> | <i>rac-1f</i> | <i>rac-1h</i> | <i>ent-1j</i> | <i>ent-1k</i> | <i>ent-1l</i> | 2a | 2b |
|-------------------------------|---------------|---------------|---------------|---------------|---------------|---------------|-----------|-----------|
| DHET production(% of vehicle) | 8.6 | 20 | 32 | 12 | 7.3 | 9.2 | 48 | 66 |

^a DHET production was measured at 1 h after the addition of 14,15-EET and compound at 1 µM concentration.

Table 4
Rat PK^a

| Compd | F (%) | Cl (mL/min/kg) | Vd _{ss} (L/kg) | T _{1/2} (h) | AUC _{po} (µM h.kg/mg) |
|---------------|-------|----------------|-------------------------|----------------------|--------------------------------|
| <i>rac-1a</i> | 61 | 47 | 3.1 | 1.5 | 0.96 |
| <i>rac-1e</i> | 49 | 1 | 0.2 | 2.6 | 20 |
| <i>Rac-1h</i> | 86 | 0.7 | 0.23 | 3.9 | 44 |
| 2b | 61 | 0.9 | 1.6 | 18 | 26 |
| 2c | 67 | 0.7 | 0.15 | 2.6 | 31 |

^a Formulation: 1 mg/mL ethanol/PEG/water (20:40:40). iv dose: 1 mg/kg (*n* = 2). po dose: 2 mg/kg (*n* = 3). Blood concentration was determined by LC/MS/MS following protein precipitation with acetonitrile.

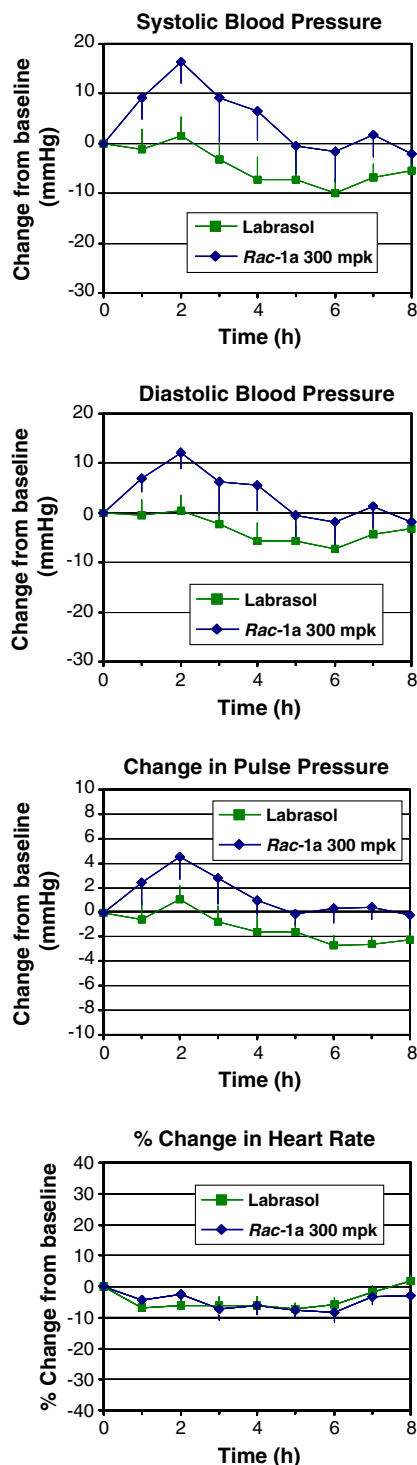
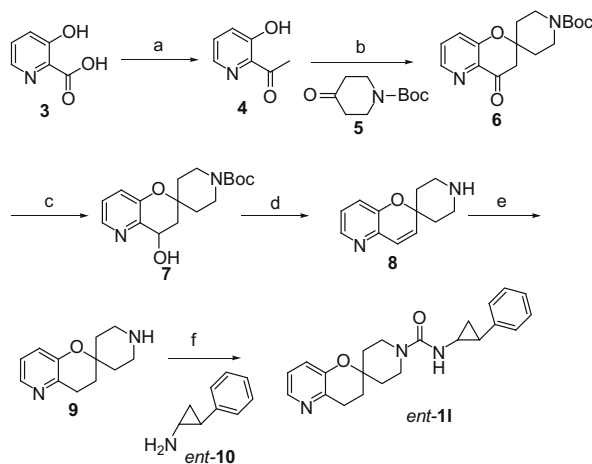


Figure 3. Blood pressure, pulse and heart rate effects of *rac-1a* in SHR (300 mpk, po) (green curve: labrasol; blue curve: *rac-1a*).

leading to *entA-1a*) to give the desired urea *ent-11*. Analogous synthetic routes led to other analogs shown in Tables 1 and 2.

In conclusion, we have identified a novel spirocyclic amine-derived urea class as potent and selective sEH inhibitors with good PK and ex vivo target engagement. However, *rac-1a*, a representative compound of this series, failed to elicit a significant blood pressure lowering effect in SHR. More structurally diverse sEH inhibitors will be reported in due course.



Scheme 1. Reagents and conditions: (a) MeMgBr, HCO₂Me, THF, reflux, 2 h, 87%; (b) pyrrolidine, 5, MeOH, reflux, 0.5 h, 75%; (c) NaBH₄, EtOH, 0 °C to rt, 2 h, 99%; (d) *p*-toluenesulfonic acid, toluene, Dean-Stark, 24 h; (e) H₂, Pd/C, MeOH, 16 h; (f) *i*-Pr₂NEt, CH₂Cl₂, *ent-10*, *p*-nitrophenyl chloroformate, 12 h, rt, then 9, 2 h, rt, 4.5% in three steps.

References and notes

- For a leading review: Newman, J. W.; Morisseau, C.; Hammock, B. D. *Prog. Lipid Res.* **2005**, 44, 1.
- Pacifici, G. M.; Temellini, A.; Giuliani, L.; Rane, A.; Thomas, H.; Oesch, F. *Arch. Toxicol.* **1988**, 62, 254.
- Yu, Z.; Xu, F.; Huse, L. M.; Morisseau, C.; Draper, A. J.; Newman, J. W.; Parker, C.; Graham, L.; Engler, M. M.; Hammock, B. D.; Zeldin, D. C.; Kroetz, D. L. *Circ. Res.* **2000**, 87, 992.
- For a leading review: Spector, A. A.; Fang, X.; Snyder, G. D.; Weintraub, N. L. *Prog. Lipid Res.* **2004**, 43, 55.
- For a leading review: Larsen, B. T.; Gutterman, D. D.; Hatoum, O. A. *Eur. J. Clin. Invest.* **2006**, 36, 293.
- Lin, W. K.; Falck, J. R.; Wong, P. Y. *Biochem. Biophys. Res. Commun.* **1990**, 167, 977.
- Fisslthaler, B.; Popp, R.; Kiss, L.; Potente, M.; Harder, D. R.; Fleming, I.; Busse, R. *Nature* **1999**, 401, 493.
- Spiecker, M.; Liao, J. K. *Arch. Biochem. Biophys.* **2005**, 433, 413.
- Gross, G. J.; Hsu, A.; Flack, J. R.; Nithipatikorn, K. *J. Mol. Cell Card.* **2007**, 42, 687.
- (a) Imig, J. D.; Zhao, X.; Zaharis, C. Z.; Olearczyk, J. J.; Pollock, D. M.; Newman, J. W.; Kim, I.-H.; Watanabe, T.; Hammock, B. D. *Hypertension* **2005**, 46, 975; (b) Jung, O.; Brandes, R. P.; Kim, I.-H.; Schmidt, R.; Hammock, B. D.; Busse, R.; Fleming, I. *Hypertension* **2005**, 45, 759; (c) Imig, J. D.; Zhao, X.; Capdevila, J. H.; Morisseau, C.; Hammock, B. D. *Hypertension* **2002**, 39, 690.
- Zhao, X.; Yamamoto, T.; Newman, J. W.; Kim, I.-H.; Watanabe, T.; Hammock, B. D.; Stewart, J.; Pollock, J. S.; Pollock, D. M.; Imig, J. D. *J. Am. Soc. Nephrol.* **2004**, 15, 1244.
- <http://www.aretetherapeutics.com>.
- Gomez, G. A.; Morisseau, C.; Hammock, B. D.; Christianson, D. W. *Protein Sci.* **2006**, 15, 58.
- (a) Delombaert, S.; Eldrup, A. B.; Kowalski, J. A.; Mugge, I. A.; Soleymanzadeh, F.; Swinamer, A. D.; Taylor, S. J. WO2007106705 A1, **2007**; (b) Ingraham, R. H. WO2007106706 A1, **2007**; (c) Hammock, B. D.; Jones, P. D.; Morisseau, C.; Huang, H.; Tsai, H.-J.; Gless, R. WO2007106525 A1, **2007**; (d) Hammock, B. D.; Kim, I.-H.; Morisseau, C.; Watanabe, T.; Newman, J. W. WO2006045119 A2, **2006**; (e) Eldrup, A. B.; Farrow, N. A.; Kowalski, J. A.; Delombaert, S.; Mugge, I. A.; Soleymanzadeh, F.; Swinamer, A. D.; Taylor, S. J. WO2007098352 A2, **2007**; (f) Takahashi, H.; Ota, T.; Kakinuma, H. WO2007043652 A1, **2007**; (g) Ota, T.; Kakahashi, H.; Kakinuma, H.; Busujima, T. WO2007043653 A1, **2007**; (h) Ingraham, R. H.; Proudfoot, J. R. WO2003002555 A1, **2003**; (i) Cardozo, M. G.; Ingraham, R. H. WO2006121684 A2, **2006**; (j) Cywin, C. L.; De Lombaert, S.; Eldrup, A. B.; Ingraham, R. H.; Taylor, S.; Soleymanzadeh, F. WO2006121719 A2, **2006**; (k) Kroetz, D.; Zeldin, D. C.; Hammock, B. D.; Morisseau, C. US20030119900 A1, **2003**; (l) Kroetz, D.; Zeldin, D. C.; Hammock, B. D.; Morisseau, C. US20040092487 A1, **2004**; (m) Hammock, B. D.; Kim, I.-H.; Morisseau, C.; Watanabe, T.; Newman, J. W. US20050026844 A1, **2005**; (n) Erickson, D.; Hoffman, A. F.; Warren, T. C. WO200023060, **2000**; (o) Hwang, S. H.; Tsai, H.-J.; Liu, J.-Y.; Morisseau, C.; Hammock, B. D. *J. Med. Chem.* **2007**, 50, 3825; (p) Kim, I.-H.; Morisseau, C.; Watanabe, T.; Hammock, B. D. *J. Med. Chem.* **2004**, 47, 2110; (q) Kim, I.-H.; Heirtzler, F. R.; Morisseau, C.; Hishi, K.; Tsai, H.-J.; Hammock, B. D. *J. Med. Chem.* **2005**, 48, 3621; (r) Morisseau, C.; Newman, J. W.; Tsai, H.-J.; Baecker, P. A.; Hammock, B. D. *Bioorg. Med. Chem. Lett.* **2006**, 16, 5439; (s) Li, H.-Y.; Jin, Y.; Morisseau, C.; Hammock, B. D.; Long, Y.-Q. *Bioorg. Med. Chem. Lett.* **2006**, 14, 6586.

15. Morisseau, C.; Newman, J. W.; Dowdy, D. L.; Goodrow, M. H.; Hammock, B. D. *Chem. Res. Toxicol.* **2001**, *14*, 409.
16. (a) Jamieson, C.; Moir, E. M.; Rankovic, Z.; Wishart, G. J. *Med. Chem.* **2006**, *49*, 5029, and references therein; (b) Fisslthaler, B.; Hinsch, N.; Chataigneau, T.; Popp, R.; Kiss, L.; Busse, R.; Fleming, I. *Hypertension* **2000**, *36*, 270; (c) Viswanathan, P. C.; Balser, J. R. *Trends Cardiovasc. Med.* **2004**, *14*, 28.
17. To the solution of methyl magnesium bromide in THF (86 mL, 3 M, 260 mmol) was added THF (100 mL). To the resulting solution at 64 °C was added a solution of 3-hydroxypicolinic acid (7.2 g, 52 mmol) and triethylamine (26 g) in 100 mL THF dropwise. The resulting mixture was heated under reflux for 2 h before it was cooled down to 5 °C. At this temperature, to the mixture was added 6.4 mL of methyl formate followed by quenching with 3 N HCl at 5 °C to pH 3–4. The mixture was extracted with THF twice. The combined THF phase was concentrated to 10 mL before the addition of 10 mL of water. The mixture continued to concentrate until the removal of THF. The aqueous solution was standing in a –10 °C refrigerator for 2 h. The resulting solid was collected by filtration and then dissolved in Et₂O. The Et₂O solution was dried over Na₂SO₄, concentrated to give **4** as a grey solid. (6.2 g, 45 mmol, 87%). The solution of **4** (6.2 g, 45 mmol), **5** (9.0 g, 45 mmol) and pyrrolidine (4.8 mL, 57 mmol) in methanol (200 mL) was heated at reflux for 20 min. After removing the solvents, the residue was purified on silica gel using 40–60% EtOAc/hexanes to afford **6** (10.7 g, 34 mmol, 75%) as a solid. To the solution of **6** (0.98 g, 3.1 mmol) in EtOH (50 mL) at 0 °C was added sodium borohydride (0.23 g, 6.2 mmol) and the resulting mixture was stirred for 2 h at rt. The reaction was quenched by the addition of saturated NaHCO₃ solution, and extracted with EtOAc twice, the combined organic phase was washed with saturated NaHCO₃ solution, dried over Na₂SO₄ to give **7** (0.98 g, 31 mmol, 99%) as an oil. To the solution of **7** (260 mg, 0.73 mmol) in 40 mL toluene was added *p*-toluenesulfonic acid (1.3 g, 7.2 mmol) and the solution was heated at reflux in a Dean-Stark trap overnight. After removing the solvent, the residue was treated with methanol (50 mL) and 10% palladium on carbon (50 mg), and the resulting suspension was subjected to hydrogenation overnight. After filtration, the solvent was removed and the residue was partitioned between 30% of isopropanol in 10% Na₂CO₃ solution. The organic phase was dried over Na₂SO₄ and concentrated to give **9** as a crude product. To the solution of *p*-nitrophenyl chlorofomate (163 mg, 0.8 mmol) in THF (5 mL) at 0 °C was added a solution of *ent*-**10** (106 mg, 0.8 mmol) and diisopropylethyl amine (180 µL, 1.0 mmol) in DCM (5 mL). After stirring overnight, the solution was transferred to a flask containing **9**. The resulting solution was stirred at rt for 2 h. After concentration, the residue was purified on silica gel chromatography using 40–100% EtOAc/hexanes to give 12 mg of *ent*-**11** (12 mg, 0.033 mmol, 4.5% overall yield in 3 steps from **7** to *ent*-**11**). ¹H NMR (acetone-*d*₆, 500 MHz) δ = 8.09–7.08 (m, 1H), 7.26–7.10 (m, 7H), 6.38 (s, 1H), 3.82 (dd, *J* = 13.0, 1.5 Hz, 2H), 3.21 (t, *J* = 10.8 Hz, 2H), 2.90 (t, *J* = 3.0 Hz, 2H), 2.83 (t, *J* = 3.2 Hz, 1H), 1.99–1.93 (m, 3H), 1.74 (d, *J* = 13.6 Hz, 2H), 1.65–1.59 (m, 2H), 1.19–1.09 (m, 2H); *m/z*: calcd. for C₂₂H₂₅N₃O₂: 363.46; found [M+H]⁺: 364.63.